

DISCOVERY OF AN EDGE-ON DUST DISK AROUND THE [WC10] CENTRAL STAR CPD $-56^{\circ}8032$

ORSOLA DE MARCO,¹ M. J. BARLOW,² AND M. COHEN³

Received 2002 May 7; accepted 2002 June 12; published 2002 June 24

ABSTRACT

We present *Hubble Space Telescope* ultraviolet and optical Space Telescope Imaging Spectrograph spectroscopy of the [WCL] planetary nebula central star CPD $-56^{\circ}8032$, obtained during its latest light-curve minimum. The UV spectrum shows the central star's continuum light distribution to be split into two bright peaks separated by $0''.10$. We interpret this finding as due to an edge-on disk or torus structure that obscures direct light from the star, which is seen primarily via its light scattered from the disk's rims or lobes. CPD $-56^{\circ}8032$ is an archetype of dual dust chemistry [WCL] planetary nebulae, which exhibit strong infrared emission features from both carbon-rich and oxygen-rich materials, and for which the presence of a disk harboring the O-rich grains had been suggested. Our direct observation of an edge-on occulting dust structure around CPD $-56^{\circ}8032$ provides strong support for such a model and for binary interactions being responsible for the correlation between the dual dust chemistry phenomenon in planetary nebulae and the presence of a hydrogen-deficient [WCL] Wolf-Rayet central star.

Subject headings: binaries: eclipsing — planetary nebulae: general — reflection nebulae — stars: AGB and post-AGB — stars: individual (CPD $-56^{\circ}8032$, He 2-113) — stars: Wolf-Rayet

1. INTRODUCTION

WC Wolf-Rayet central stars ([WC] CSs) of planetary nebulae (PNs) are H-deficient stars that exhibit strong ionic emission lines of helium, carbon, and oxygen from their dense stellar winds. Among the coolest central stars in this group are CPD $-56^{\circ}8032$ (the nucleus of the PN He 3-1333) and the CS of He 2-113 (both classified as [WC10]; Crowther, De Marco, & Barlow 1998). Cohen et al. (1986) found the mid-infrared Kuiper Airborne Observatory spectra of both these objects to show very strong unidentified infrared bands (UIBs; usually attributed to polycyclic aromatic hydrocarbons). Indeed, both the nebular C/O ratios (De Marco, Barlow, & Storey 1997) and the ratio of UIB luminosity to total IR dust luminosity (Cohen et al. 1989) for these two objects are among the largest known. It was therefore a major surprise when mid- and far-IR *Infrared Space Observatory* spectra of these two objects showed the presence of many emission features longward of $20\ \mu\text{m}$ that could be attributed to crystalline silicate and water ice particles (Barlow 1997; Waters et al. 1998a; Cohen et al. 1999), indicating a dual dust chemistry, i.e., the simultaneous presence of both C-rich dust and O-rich dust. The dual dust chemistry phenomenon in PNs appears to show a strong correlation with the presence of a late WC ([WCL]) nucleus—four out of six [WC8–11] nuclei studied by Cohen et al. (2002) showed similar dual dust chemistries. In the context of a single-star scenario, this would point to a recent transition (within the last ~ 1000 yr) between the O-rich and the C-rich surface chemistries. However, the probability of finding a post-asymptotic giant branch (AGB) object that had recently changed from an O-rich to a C-rich surface chemistry owing to a third dredge-up event should be very low indeed. An alternative scenario envisages these systems as binaries (Waters et al. 1998a; Cohen et al. 1999, 2002), in which the O-rich silicates are trapped in a disk as a result of a past mass transfer

event, with the C-rich particles being more widely distributed in the nebula as a result of recent ejections of C-rich material by the nucleus. Because of the quasi-periodic light variations shown by CPD $-56^{\circ}8032$, Cohen et al. (2002) suspected the presence of a precessing disk around it. In this Letter, we present the first direct evidence for an edge-on disk or torus around CPD $-56^{\circ}8032$, as revealed by recent *Hubble Space Telescope* (*HST*) Space Telescope Imaging Spectrograph (STIS) spectroscopy.

2. OBSERVATIONS

STIS/*HST* observations of CPD $-56^{\circ}8032$ (and of He 2-113 and SwSt 1; O. De Marco et al. 2002, in preparation) were obtained on 2001 April 1–5, when the star was in its third recorded visual light minimum ($V \sim 12.5$ mag; Cohen et al. 2002). The MAMA+G230L grating ($R \sim 740$, $\lambda = 1570\text{--}3180\ \text{\AA}$, exposure time 2200 s), CCD+G430M grating ($R \sim 6600$, $\lambda = 3540\text{--}3820\ \text{\AA}$, exposure time 1120 s), and CCD+G750L grating ($R \sim 800$, $\lambda = 5240\text{--}10270\ \text{\AA}$, exposure time 910 s) were used together with the 52×0.2 arcsec² aperture. In the top panel of Figure 1, we present the two-dimensional MAMA spectral image of CPD $-56^{\circ}8032$ ($0''.024$ pixel⁻¹ in the spatial direction). For comparison, we also present similar observations made of the [WC10] nucleus of He 2-113 and its nebula (*bottom*). In Figure 2, we present the long-pass filter ($>5500\ \text{\AA}$) CCD acquisition images (F28X50LP; $0''.050$ pixel⁻¹) for both objects. The slit was oriented with a position angle (P.A.) of 243° for CPD $-56^{\circ}8032$ and 300° for He 2-113. The near-UV spectral image of He 2-113 in Figure 1 shows a spatially unresolved continuum attributable to the central star, while that of CPD $-56^{\circ}8032$ shows the continuum light distribution to be split into two bright peaks separated by $0''.10$, together with a third, weaker peak displaced by $0''.3$ to the northeast. In the much longer wavelength direct image of CPD $-56^{\circ}8032$, such structure cannot be resolved. The morphology of CPD $-56^{\circ}8032$ (Fig. 2) is highly uncertain (the only previous *HST* images were pre-COSTAR; De Marco et al. 1997). If any symmetry axis is present, it lies at about P.A. $\sim 10^{\circ}$, in which case the slit P.A. would lie at about 50° to the symmetry axis. Our long-pass filter acquisition image appears to be at too long a wavelength (central wavelength $\sim 7200\ \text{\AA}$)

¹ Department of Astrophysics, American Museum of Natural History, Central Park West at 79th Street, New York, NY 10024.

² Department of Physics and Astronomy, University College London, Gower Street, London WC1E 6BT, UK.

³ Radio Astronomy Laboratory, University of California at Berkeley, 601 Campbell Hall, Berkeley, CA 94720.

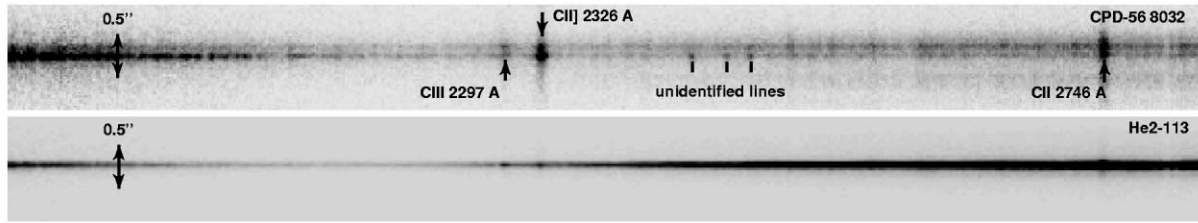


FIG. 1.—STIS/MAMA two-dimensional spectra of the planetary nebulae He 3-1333 (*top*; central star = CPD $-56^{\circ}8032$ = V837 Ara) and He 2-113 (*bottom*; central star = He 3-1044).

for any preferred axis to be discernible in the extended profile of the central object.

3. RESULTS

In Figure 3, we present spatial crosscuts (where 10 MAMA/CCD columns were averaged) through the CPD $-56^{\circ}8032$ and He 2-113 spectra, centered at different wavelengths. The spatial profile through He 2-113's central star is very close to that expected for the MAMA+G140L and CCD+G430M and G750L point-spread functions (as detailed in the STIS handbook), while CPD $-56^{\circ}8032$ exhibits a much broader profile, which in the MAMA spectrum is dominated by two peaks separated by 4 pixels = $0''.096$. The similarity of the spatial distribution of CPD $-56^{\circ}8032$'s stellar continuum, at 3107 \AA (MAMA) and at 3700 \AA (CCD), implies that the splitting observed in the MAMA spectrum is not due to an observational peculiarity. The Figure 3 MAMA crosscuts show the northeasterly of the two sharp peaks to be brighter at the shortest UV wavelengths, with the southwesterly peak brightening to be stronger at the longest UV wavelengths. The two main peaks seen in the UV are no longer resolved in the CCD optical crosscuts, owing to the 2 times larger dimensions of the $0''.05$ CCD pixels and the linear increase with wavelength of the *HST*'s diffraction-limited angular resolution ($0''.093$ at 8906 \AA). The acquisition image has a filter central wavelength of 7200 \AA , and the profile of its P.A. = 243° crosscut appears intermediate between those that we made at 5412 and 8906 \AA in the CCD spectral image. The CPD $-56^{\circ}8032$ spatial profile at 8906 \AA is only slightly broader than that for He 2-113, indicating that CPD $-56^{\circ}8032$'s central star is maybe being seen directly at that

wavelength, with the reflected light components having decreased significantly in intensity.

From Figure 3, it is clear that the reflected light spectrum is a function of spatial position. In particular, to the northeast, at about $-0''.3$, the reflected light increases in intensity at around 3000 \AA , relative to the two main peaks (see the 2881 \AA crosscut in Fig. 3). We also note that the lower of the two principal reflected continuum peaks exhibits three unidentified emission lines, at 2439 , 2466 , and 2483 \AA (see Fig. 1, *top*), indicating that an emission component, perhaps fluorescent, must be present in addition to the stellar scattered light component. The detailed spectral properties of the individual regions discernible in our STIS spectral images will be discussed elsewhere.

A comparison between $1800\text{--}3200 \text{ \AA}$ low-resolution *International Ultraviolet Explorer* (*IUE*) spectra taken in 1979–1980, 1987 July, and 1991 August shows the *IUE* spectra all to have had identical spectral shapes, although the absolute flux levels in 1987 and 1991 were 0.72 and 0.80 of those in 1979–1980 (the *UBV* photometry of Pollacco et al. 1992 shows that CPD $-56^{\circ}8032$ was at its maximum brightness level when the 1991 August *IUE* spectra were acquired). A summation of all the main emission regions discernible along the length of the $0''.2$ wide MAMA slit (extracted using a 158 pixel wide aperture between pixel 590 and 679 in the two-dimensional STIS image) yielded a spectrum that longward of 2200 \AA has the same spectral shape as the *IUE* spectra but that becomes progressively bluer than the *IUE* spectra shortward of 2200 \AA . A change in stellar parameters is excluded by the fact that the UV and optical stellar emission lines in the STIS spectra have very similar equivalent widths to those measured on the *IUE* and Anglo-Australian Telescope

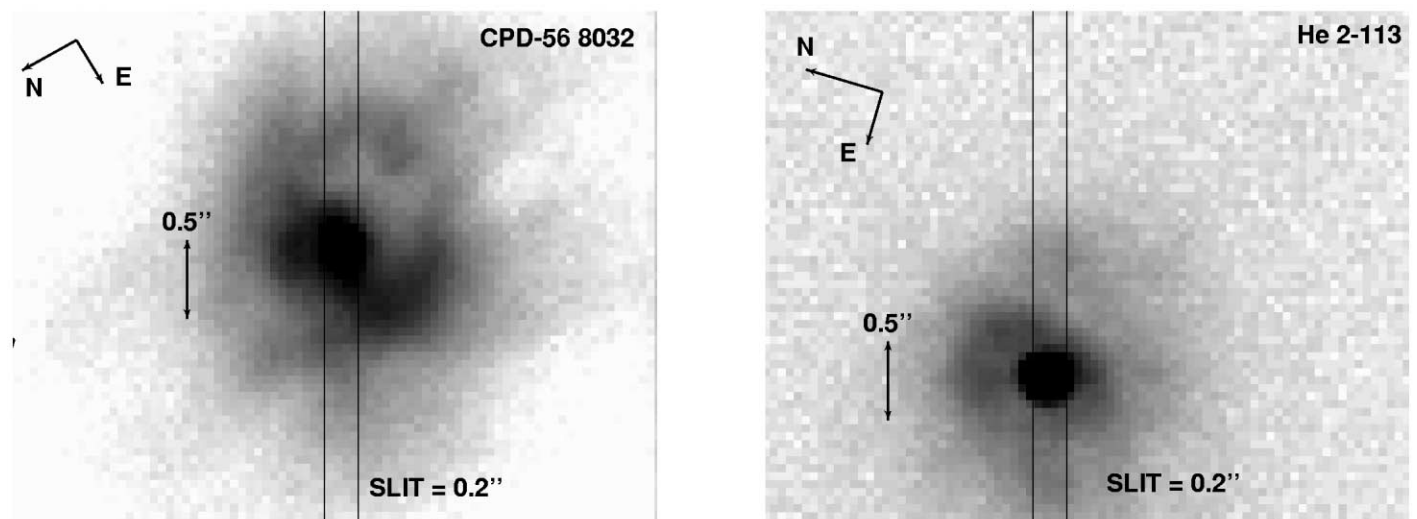


FIG. 2.—STIS long-pass filter ($\lambda > 5500 \text{ \AA}$) acquisition images. Exposure times are 5.8 s for CPD $-56^{\circ}8032$ (*left*) and 3 s for He 2-113 (*right*).

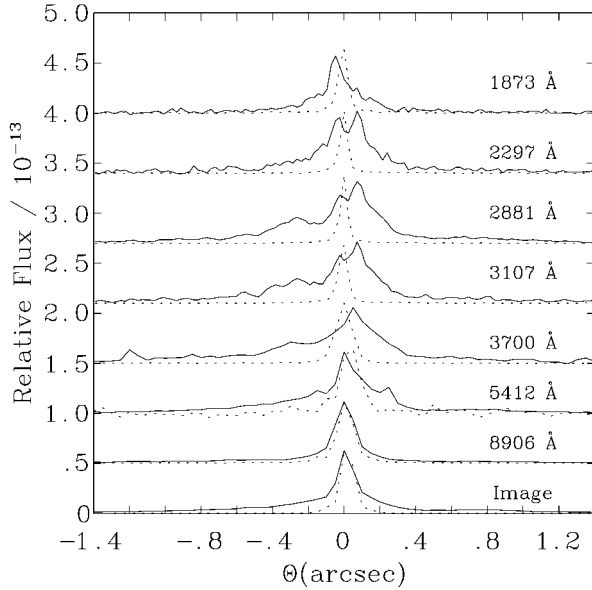


FIG. 3.—STIS/MAMA and CCD crosscuts in the spatial direction, comparing CPD $-56^{\circ}8032$'s intensity distribution (*solid lines*) to that of He 2-113 at the same wavelength (*dotted lines*; scaled to CPD $-56^{\circ}8032$'s peak intensity). The wavelength of each cut is indicated. CPD $-56^{\circ}8032$'s cuts are normalized to the peak intensity at 2297 Å, and the zero levels are successively incremented by 0.5×10^{-13} ergs cm^{-2} s^{-1} Å $^{-1}$. The bottom curve is a cut at P.A. = 243° through the acquisition image ($\lambda > 5500$ Å; central wavelength 7200 Å).

spectra of De Marco et al. (1997). However, a more detailed comparison between the *IUE* and STIS spectra is hindered by the fact that the area of the 20×10 arcsec 2 *IUE* entrance aperture was considerably larger than that of the $0''.2$ wide STIS long slit used in 2001 May, so that the latter is likely to have sampled only a fraction of the total emission—longward of 2200 Å the continuum flux level in the summed MAMA spectrum is 18 times lower than that in the 1979–1980 *IUE* spectra.

4. DISCUSSION

Our working hypothesis is that the observed spatial splitting of CPD $-56^{\circ}8032$'s continuum (Figs. 1 and 3) is due to obscuration of the central object by a dusty disk or torus seen close to edge-on. Under this interpretation, the two continuum peaks separated by $0''.10$ are attributed to scattered light emerging from the upper and lower rims of the disk/torus, or from two lobes residing above and below the disk/torus, resembling the edge-on structure observed in the Red Rectangle, HD 44179 (Osterbart, Langer, & Weigelt 1997), or the edge-on silhouette disk Orion 114–426 (McCaughrean et al. 1998). It seems possible that the STIS slit was oriented nearly normal to the P.A. of the disk, in agreement with the slit P.A. being only $\sim 50^{\circ}$ from the inferred axis of symmetry of the nebula. Our 2001 May STIS spectrum was obtained during a light minimum of CPD $-56^{\circ}8032$, the latest of three observed visual light declines having an apparent periodicity of ~ 5 yr (Cohen et al. 2002). Cohen et al. suggested that these light declines could be due to the precession of a nearly edge-on obscuring disk, or alternatively, that they could be due to occultations of the central object by particularly dense clumps orbiting within the disk, in which case the apparent periodicity might be accidental. One might argue that CPD $-56^{\circ}8032$'s light variations could be due to random dust ejections, similar to those of R Coronae Borealis (R CrB) stars. Although CPD $-56^{\circ}8032$'s apparent

5 yr period can be confirmed only by more observations, we note that R CrB light declines are much deeper (~ 8 mag) and always associated with spectral variability (Clayton 1996). Even V348 Sgr (a [WC]-like CS not dissimilar to CPD $-56^{\circ}8032$; Leuenhagen, Heber, & Jeffery 1994) has deep declines and spectral variability, similarities to R CrB characteristics that are not shared by CPD $-56^{\circ}8032$. Finally, resolved occulting structures, of the type found here around CPD $-56^{\circ}8032$, have never been detected around R CrB stars.

As an alternative to disk precession being responsible for CPD $-56^{\circ}8032$'s visible light variability, the orbital motion of the star itself (clearly, we have to assume the presence of a binary companion) might bring it in and out of alignment with a denser region in the disk. A similar behavior has been inferred by Van Winckel et al. (1999) for the binary post-AGB objects HD 52961 and HR 4049, for both of which circumstellar extinction variations were found to occur on the same timescales as the respective binary orbital periods of 1310 and 429 days, although we note that their optical extinction variations show amplitudes of only 0.16–0.20 mag, versus 1.6 mag for CPD $-56^{\circ}8032$. If we assume the alleged companion star to have a similar mass to CPD $-56^{\circ}8032$ (and that both have masses of $0.6 M_{\odot}$), the orbital semimajor axis, for a circular orbit, would be 3.1 AU. The $0''.10$ angular separation between the two main scattered light components in the MAMA spectral image are assumed to correspond to the top and bottom edges of a disk or torus with a projected disk semithickness of 67 AU (for a distance of 1.35 kpc; De Marco et al. 1997) or to two lobes residing at 67 AU above and below the disk/torus. Cohen et al. (1999) estimated the 65–90 K oxygen-rich grains around CPD $-56^{\circ}8032$ to lie 1000 AU from the star, but this was based on an optically thin assumption. Our present results indicate that these cool O-rich grains are likely to be located much closer to the star, in the outer regions of an optically thick edge-on reprocessing disk. As noted above, a similar structure to that of CPD $-56^{\circ}8032$ is observed around the HD 44179 nucleus of the Red Rectangle, a non-H-deficient post-AGB object that was found by Waters et al. (1998b) to exhibit a dual dust chemistry. Inspection of Figures 2 and 3 of Cohen et al. (2002) shows the long-wavelength peak of CPD $-56^{\circ}8032$'s infrared energy distribution to lie at the same wavelength as those of the three other [WCL] objects plotted, but also that this peak is much weaker relative to the $7.7 \mu\text{m}$ UIB-like feature than is the case for the other three objects. If the crystalline silicate and long-wavelength continuum emission originates from an orbiting disklike region around each object, then this effect could be due to CPD $-56^{\circ}8032$'s disk being viewed edge-on, thereby significantly reducing the amount of radiation received from its disk.

One remaining issue to be considered is the very strong association between the dual dust chemistry phenomenon in PNs and the presence of an H-deficient central star and what that might tell us about a common cause for the two phenomena. We might expect that some [WC] stars are single and simply evolve to be a [WC] CS as a result of the well-timed thermal pulses described by Herwig (2001), in which case they would not be expected to exhibit dual dust chemistries. Indeed, several [WCL] PNs show no evidence for dual dust chemistries (Cohen et al. 2002; Hony, Waters, & Tielens 2001) and may well have originated via the well-timed thermal pulse mechanism. However, the current evidence points to binarity playing a key role in the origin of at least some H-deficient [WCL] nuclei and the dual dust chemistry phenomenon, with mass transfers first leading to the creation of a massive circumbinary disk and later stripping most or all of the H-rich surface layer

from the CS progenitor. Under this scenario, the B9/A0 III central star of the Red Rectangle might be interpreted as possessing only a very thin surface hydrogen layer, which will quickly be stripped away to yield an H-deficient [WCL] nucleus once the stellar effective temperature increases to high enough values ($>20,000$ K) for radiation pressure driven mass loss to become significant.

To conclude, our STIS observations indicate the presence of an edge-on occulting dust structure in the CPD $-56^{\circ}8032$ system—further observations will be needed to determine how its appearance changes as the star returns to maximum. It would also be desirable for the orbital characteristics of the inferred

CPD $-56^{\circ}8032$ binary system to be determined directly via radial velocity measurements of the [WC10] star's emission lines. Similar radial velocity measurements should also be obtained for the central stars of other dual dust chemistry [WCL] PNs, even if, as is likely in the case of He 2-113, the possible dust disks are not oriented edge-on to us.

O. D. gratefully acknowledges Janet Jeppson Asimov for financial support. O. D. and M. C. acknowledge support from NASA grant HST-GO-08711.05-A. Our thanks go to Paul Goodfroy, STIS scientist, for helping us to understand the instrumental intricacies of STIS.

REFERENCES

- Barlow, M. J. 1997, *Ap&SS*, 255, 315
 Clayton, G. C. 1996, *PASP*, 108, 401
 Cohen, M., Allamandola, L., Tielens, A. G. G. M., Bregman, J., Simpson, J. P., Witteborn, F. C., Wooden, D., & Rank, D. 1986, *ApJ*, 302, 737
 Cohen, M., Barlow, M. J., Liu, X.-W., & Jones, A. F. 2002, *MNRAS*, 332, 879
 Cohen, M., Barlow, M. J., Sylvester, R. J., Liu, X.-W., Cox, P., Lim, T., Schmitt, B., & Speck, A. K. 1999, *ApJ*, 513, L135
 Cohen, M., Tielens, A. G. G. M., Bregman, J. D., Allamandola, L. J., Wooden, D., & Jourdain de Muizon, M. 1989, *ApJ*, 341, 246
 Crowther, P. A., De Marco, O., & Barlow, M. J. 1998, *MNRAS*, 296, 367
 De Marco, O., Barlow, M. J., & Storey, P. J. 1997, *MNRAS*, 292, 86
 Herwig, F. 2001, *Ap&SS*, 275, 15
 Hony, S., Waters, L. B. F. M., & Tielens, A. G. G. M. 2001, *A&A*, 378, L41
 Leuenhagen, U., Heber, U., & Jeffery, C. S. 1994, *A&AS*, 103, 445
 McCaughrean, M. J., et al. 1998, *ApJ*, 492, L157
 Osterbart, R., Langer, N., & Weigelt, G. 1997, *A&A*, 325, 609
 Pollacco, D. L., Kilkenny, D., Marang, F., van Wyck, F., & Roberts, G. 1992, *MNRAS*, 256, 669
 Van Winckel, H., Waelkens, C., Fernie, J. D., & Waters, L. B. F. M. 1999, *A&A*, 343, 202
 Waters, L. B. F. M., et al. 1998a, *A&A*, 331, L61
 ———. 1998b, *Nature*, 391, 868